High-pressure Raman study of the ternary chalcogenides $TlGaS_2$, $TlGaSe_2$, $TlInS_2$, and $TlInSe_2$

W. Henkel, H. D. Hochheimer, C. Carlone,* A. Werner, S. Ves,† and H. G. v. Schnering
Max-Planck-Institut für Festkörperforschung, Heisenbergstrasse 1, D-7000 Stuttgart 80, Federal Republic of Germany

(Received 21 December 1981; revised manuscript received 10 May 1982)

The Raman spectra of tetragonal $TlInSe_2$ and monoclinic $TlGaS_2$, $TlGaSe_2$, and $TlInS_2$ have been investigated as a function of pressure at constant temperatures (300 and 110 K, $TlInSe_2$ only at 110 K). Contrary to earlier assignment the structure of the monoclinic compounds can be described in the space group $C2/c$. The appearance and disappearance of Raman modes with increasing pressure are due to a crossing of bands with A_g and B_g symmetry and do not indicate the occurrence of a structural phase transition. In $TlInS_2$ we observe modes with a negative pressure dependence indicating an impending phase transition at pressures above the maximum pressure of our measurements. The dependence of $(1/\nu)(d\nu/dp)$ on ν of the observed Raman bands in these compounds reveals that a hierarchy of bonding forces is present.

I. INTRODUCTION

The ternary semiconducting chalcogenides with the formula ABX_2 (A,B represent metal atoms, X represents chalcogen atoms) have been studied intensively in recent years.[1–16] In this study we have investigated the thallium chalcogenides $TlBX_2$ ($B \equiv$ Ga,In; $X \equiv$ S,Se) under ambient as well as high pressure to resolve the controversies concerning their structure as well as possible phase transitions and their lattice dynamics.

Zallen[17] has shown that the mode-Grüneisen parameters obtained from Raman data reflect the distribution of forces in a molecular or layered crystal. Furthermore, an impending phase transition is often indicated by the pressure dependence of certain modes.[18] Therefore, we felt a high-pressure Raman study of the ternary chalcogenides $TlGaS_2$, $TlGaSe_2$, and $TlInS_2$ and $TlInSe_2$ could provide the information.

Our study has shown that there is a hierarchy of bonding forces. Also the disappearance and appearance of Raman bands with increasing pressure is not due to a structural phase transition, as reported by Vinogradov *et al.*[15] in the case of $TlGaSe_2$ and $TlGaS_2$. Rather, the observed effects can be explained by a crossing of modes of A_g and B_g symmetry.

II. EXPERIMENTAL

All compounds were grown from high-purity elements (at least 99.999%). Stoichiometric portions of the materials were sealed into an evacuated ($\sim 10^{-5}$-Torr) silica-glass tube which then was heated above the melting point of the compounds, in steps of about 50 °C every 10 h. The melts were held at about 5–10 °C above the melting temperature for 2–3 days, then shaken vigorously several times to ensure thorough mixing. After this treatment the melts were cooled slowly to 5 °C below the melting point and held at that temperature for two weeks. Then they were temperature quenched by suddenly immersing the glass tube into cold water. The crystals obtained by this treatment were heavily twinned, but exhibited good optical quality and could easily be cleaved into plates parallel to (001).

Samples of about 50 μm in linear dimensions cut from these crystals were used for the Raman measurements. Pressure was generated in a high-pressure diamond-anvil cell. An Inconel gasket with a 200-μm hole served as the pressure chamber. The sample together with a small ruby chip was placed inside the hole and then the chamber was filled with the usual 4:1 methanol-ethanol mixture as pressure medium. The pressure was measured by the well-known ruby fluorescence technique.[18] For temperature-dependent studies the diamond cell could be cooled down to 110 K in a bath cryostat. All Raman spectra were recorded with the usual Raman equipment in backscattering geometry. The experiments were performed with the 647.1-nm line of a krypton laser. The typical laser power was about 50 to 100 mW.

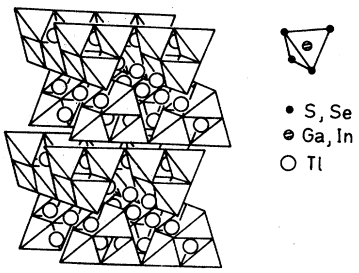

FIG. 1. Stacking of the anionic layers and positions of Tl^+ ions between them.

In all the compounds, increasing pressure caused a darkening of the samples and a decrease in the Raman intensities until the Raman bands finally vanished in the background. For each compound this darkening was responsible for limiting the values of the highest pressure attained in these measurements.

III. CRYSTALLOGRAPHIC DATA AND RESULTS OF THE GROUP-THEORETICAL ANALYSIS

We show in Fig. 1 the stacking of the anionic layers and the positions of the Tl^+ ions between the anionic layers. The B_4X_{10} polyhedra (B represents metal atoms, X represents chalcogen atoms) are built up adamantinelike by four BX_4 tetrahedra with common corners. In addition, these B_4X_{10} polyhedra are condensed with four neighboring polyhedra by common corners forming a $^2_\infty(BX_2)$ layer parallel to (001) (see Fig. 1). The upper and lower edges of these adamantinelike units point in the [110] and [$\bar{1}$10] directions. Two such layers are stacked in the cell along [001]. Succeeding layers are twisted 90° to each other forming trigonal prismatic voids. The Tl^+ ions are positioned in these trigonal prisms between the layers arranged on straight lines parallel to [110] and [$\bar{1}$10]. The stereographic projection of the structure (Fig. 2) reveals the above-mentioned features more completely by showing all the atoms.

The confusing variety of data on the structure, space group, and lattice constants arise from the following. Our own investigations as well as that of Müller, Poltmann, and Hahn[4] have shown that in these compounds the formation of twins simulates a length of the c axis of about 30 Å. From this one can eliminate all unit-cell data with a value of about 30 Å for the c axis.[1,8,10,11] The formation of twins is also responsible for the fact that the monoclinic symmetry was overlooked and tetragonal symmetry was erroneously assigned.[1,6,11] Furthermore, assuming a tetragonal description, a pseudotetragonal cell with $a=b\approx 7.7$ Å is equivalent to a pseudotetragonal cell with $a'=b'=a\sqrt{2}\approx 10.9$ Å, which is the projection of the monoclinic cell with $\beta=100°$ (Refs. 4 and 7). In the case of $TlInSe_2$ we really have a tetragonal TlSe-type structure. As this has led to speculations about the symmetry of the layer in the monoclinic compounds, we like to emphasize that the tetragonal structure of $TlInSe_2$ is completely different from the one assumed for the so-called "tetragonal" monoclinic ternary chalcogenides. Taking into account the above-mentioned facts, we have compiled from literature data in Table I a correct set of crystallographic data for the four compounds.

Müller and Hahn[7] have overlooked in their structure the presence of inversion centers. Thus they have assigned the lower symmetry (Cc) to the monoclinic ternary chalcogenides. Based on the data of Müller and Hahn[7] and including the inversion centers, we assign the space group $C2/c$ to these compounds (see Sec. II). This assignment is in agreement with results obtained by Gasanly *et al.*[14] [relatively small number of Raman bands in spite of the complex crystal structure (64 atoms in the elementary cell), no coincidence of Raman- and infrared-active bands, and negative piezoelectric test].

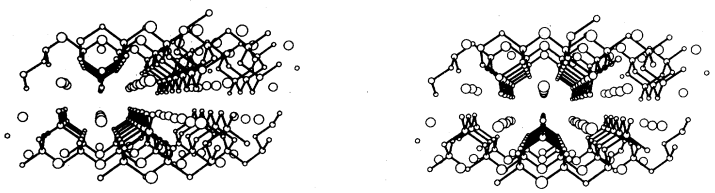

FIG. 2. Stereographic representation of the structure of $TlGaSe_2$.

TABLE I. Crystallographic data of $TlGaS_2$, $TlGaSe_2$, $TlInS_2$, and $TlInSe_2$.

Compound	Reference	Structure	Space group	Lattice constants a (Å)	b (Å)	c (Å)	β or c/a	Z
$TlGaS_2$	4	monoclinic	$C2/c$-C_{2h}^6	10.40	10.40	15.17	100°	16
$TlGaSe_2$	7	monoclinic	$C2/c$-C_{2h}^6	10.772(3)	10.771(5)	15.636(8)	100.06(3)°	16
$TlInS_2$	4	monoclinic	$C2/c$-C_{2h}^6	10.95	10.95	15.14	100°	16
$TlInSe_2$	11	tetragonal	$14/mcm$-D_{4h}^{18}	8.02	a	6.826	0.85	4

At the moment reliable x-ray data of the atom coordinates[7] are only available for $TlGaSe_2$. From the given atomic positions we have determined a center of symmetry to be at $x=0.0255$, $y=0$, $z=0.1237$. All positions are in agreement with the higher-symmetry $C2/c$ and stay with respect to this center within the range of the standard deviations listed in Ref. 7. We think that this fact as well as the facts mentioned earlier overrule the assignment of the space group Cc supported only by a statistical intensity test. In Table II we have listed the atomic positions of $TlGaSe_2$ in the space group $C2/c$. The unit cell contains 16 formula units of $TlGaSe_2$ (two layers), but the primitive cell 8 units in the two layers, because of the C centering. A layer in the primitive cell is built up from 2 Tl1, 2 Tl2, 2 Ga1, 2 Ga2, 1 Se1, 1 Se2, 2 Se3, 2 Se4, 2 Se5, and has the site symmetry C_2. A factor-group analysis based on the type of grouping in the Wyckoff notation (e and f) for the atoms listed in Table II and the layers in e (site symmetry C_2), yields the following result:

$$\Gamma_{\text{red}}=23\,A_g+25\,B_g+23\,A_u+25\,B_u\ ,$$

where A_u+2B_u and A_g+2B_g are the acoustic modes and the optical interlayer modes, respectively. All others are internal vibrations of the layers. The A_g and B_g vibrations are Raman-active and the A_u and B_u vibrations are infrared-active. Thus, there are maximal 23 A_g and 25 B_g modes. This is in good agreement with experimental results of Allakhverdiev *et al.*[16] They have measured polarized Raman spectra of $TlGaS_2$ using a scattering geometry allowing Raman bands of only one symmetry species. They could resolve 17 A_g modes and have reported that the A_g and B_g spectra are practically the same. In the next section we will return to this point and discuss it in detail.

IV. RESULTS AND DISCUSSION

Although the Raman spectra of the substances we have studied have already been published, it is useful to show them for comparison of the figures and tables for each substance studied (the modes are numbered in the figures and in the tables). In Fig. 3, the room-temperature Raman spectra of $TlGaS_2$ at 0 and 3.1 GPa together with those at 110 K at 0 and 2.4 GPa are shown.

Using the results of the pressure dependence of the Raman-active modes of $TlGaS_2$ (Figs. 4 and 5), we see that some of the bands clearly consist of two or even more overlapping bands (at 300 K: band 1,2; 8,9; at 110 K: band 3,4,5; 8,9; 15,16).

TABLE II. Atomic parameters of $TlGaSe_2$ in the space group $C2/c$. The parameters were obtained by transforming and averaging the atomic positions given in Ref. 7.

Atom	Site	x'	y'	z'	Notation in Ref. 7
8 Tl1	8f	0.4632	0.1885	0.1078	Tl1 + Tl3
8 Tl2	8f	0.2163	0.0613	0.6158	Tl2 + Tl4
8 Ga1	8f	0.3981	0.1880	0.8378	Ga1 + Ga4
8 Ga2	8f	0.1461	0.0639	0.3391	Ga2 + Ga3
4 Se1	4e	0	0.9295	$\frac{1}{4}$	Se3
4 Se2	4e	0	0.4468	$\frac{1}{4}$	Se4
8 Se3	8f	0.2047	0.4370	0.0695	Se1 + Se8
8 Se4	8f	0.2588	0.1882	0.2508	Se2 + Se6
8 Se5	8f	0.4541	0.3124	0.5732	Se5 + Se7

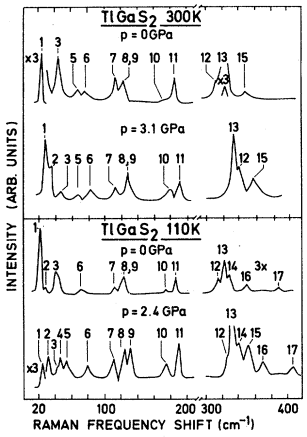

FIG. 3. Raman spectra of $TlGaS_2$ at zero and high pressure at 300 and 110 K. (Numbers correspond to the listing in Table III.)

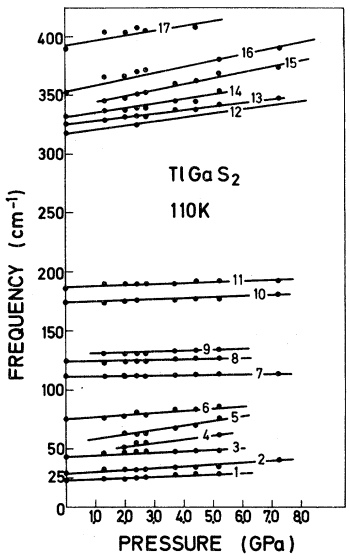

FIG. 5. Pressure dependence of the mode frequencies of $TlGaS_2$ at 110 K. (Numbers correspond to the listing in Table III.)

Furthermore, we find that at 300 K the bands 5,6 and 12,13 and at 110 K the bands 3,4 and 12,13,14,15 are crossing each other. With increasing pressure the modes clearly separate. This shows that the appearance of additional bands with increasing pressures does not necessarily mean a structural phase transition but it could be due to crossing of modes of different symmetry.

The general features of the Raman spectra of the isotypic selenide $TlGaSe_2$ are similar. Nevertheless, to enable a comparison with results of Vinogradov *et al.*[15] the room-temperature Raman spectra of $TlGaSe_2$ in the low-frequency region at pressures of 0, 0.28, and 0.66 GPa are shown in Fig. 6. Contrary to their results, we find no indication for a structural phase transition.

Figures 7 and 8 shown the pressure dependence of the mode frequencies at 300 and 110 K, respectively. Again, crossing of modes (bands 4 and 7 in

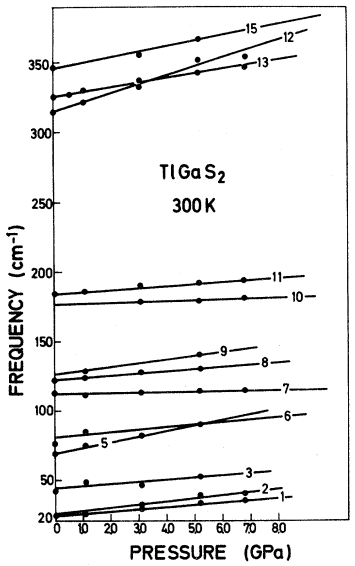

FIG. 4. Pressure dependence of the mode frequencies of $TlGaS_2$ at 300 K. (Numbers correspond to the listing in Table III.)

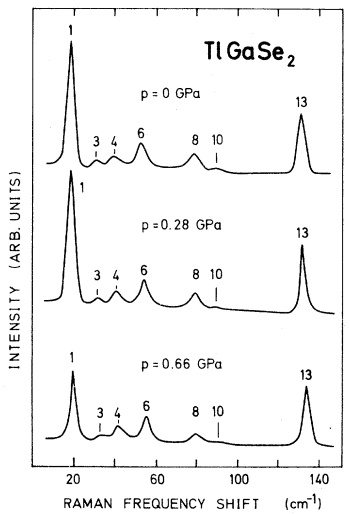

FIG. 6. Low-frequency Raman-active modes of $TlGaSe_2$ at zero, 2.83, and 6.6 kbar at 300 K. (Numbers correspond to the listing in Table IV.)

TABLE III. Raman frequencies ν_i and $(1/\nu_i^c)(d\nu_i/dP)$ of the modes in $TlGaS_2$ at low temperatures and at room temperature. ν_i^m are taken from our measurements. The values ν_i^c are determined by fitting the pressure data with a least-squares fit to $\nu_i(P)=\nu_i^c+(d\nu_i/dP)P$.

Number of the mode	ν_i (Ref. 14) (cm^{-1}) 300 K	ν_i (Ref. 15) (cm^{-1}) 300 K	ν_i (Ref. 16) (cm^{-1}) 85 K	ν_1 (cm^{-1}) 110 K	ν_1 (cm^{-1}) 300 K	ν_i^c (cm^{-1}) 110 K	ν_i^c (cm^{-1}) 300 K	$\frac{1}{\nu_i^c}\frac{d\nu_i}{dP}$ (10^{-2} GPa^{-1}) 110 K	$\frac{1}{\nu_i^c}\frac{d\nu_i}{dP}$ (10^{-2} GPa^{-1}) 300 K	$\frac{1}{\nu_i^c}\frac{d\nu_i}{dP}$ (10^{-1} GPa^{-1}) (Ref. 15) 300 K
1	22	22	21	23	23	21.4 ±0.9	23.2 ±0.6	8.5	7.7	4.6
2	29	28	29	29		28.4 ±0.5	26.2 ±3.1	6.0	8.0	8.6
3	44	43	41	42	44	43.3 ±0.8	45.9 ±1.6	2.9	0.3[a]	6.1
4	52		46			45.8 ±2.1		6.9		
5	66		72		70	50.0 ±1.9	70.0 ±0.4	9.7	5.4	
6	76		77	76	76	74.7 ±1.0	70.1 ±0.4	3.0	5.4	
7	112	113	112	112	113	111.1 ±0.4	112.0 ±0.8	0.2	0.3	−1.0
8	122	121	121	123	122	121.1 ±1.0	122	1.3	1.2	1.2
9		125	125			126.9 ±1.8	122.6 ±3.0	1.7	2.5	1.8
10	143, 150		174	173		173.0 ±0.5	176.4 ±1.3	0.6	0.3	
11	182	185	185	185	184	187.4 ±0.8	184.7 ±0.7	0.5	0.7	0.8
12	208, 224, 239 310		314 319	318	316	318	317.1 ±2.2	0.9	1.9	
13	322	324	327	325	323	325.3 ±0.6	324.5 ±1.3	0.9	1.0	2.9
14			333	331		331.0 ±1.1		1.2		
15	348	350	348		347	338.9 ±1.5	346.3 ±2.3	1.5	1.1	1.2
16			352	352		356.0 ±2.5		1.3		
17	386		391	390	386	394.9 ±3.1		0.9		

[a]This value has an extremely large error (±1.4).

TABLE IV. Raman frequencies ν_i and $(1/\nu_i^c)d\nu_i/dP$ of the modes in $TlGaSe_2$ at low temperatures and at room temperature. The values ν_i^m are taken from our measurements, those of ν_i^c are determined by fitting the pressure data with a least-squares fit to $\nu_i(P)=\nu_i^c+(d\nu_i/dP)P$.

Number of the mode	ν_i (Ref. 12) (cm^{-1})			ν_i (Ref. 14) (cm^{-1})	ν_i (Ref. 15) (cm^{-1})	ν_i^m (cm^{-1})			ν_i^c (cm^{-1})		$(1/\nu_i^c)d\nu_i/dP$ (10^{-2} GPa^{-1})		$(1/\nu_i)d\nu_i/dP$ (Ref. 15) (10^{-2} GPa^{-1})
	4 K	85 K	300 K	300 K	300 K	52 K	110 K	300 K	110 K	300 K	110 K	300 K	300 K
1	20	20	20	20	20	20	20	19[a]/19	20.3±0.5	18.2±0.5	12.0	12.1	1.8
	22.5												
2	26					26							
	29												
3	32	33	32	33	32	32	32	32[a]/31	31.1±0.3	30.6±0.1	4.2	9.5	8.3
3a	37								35.1±0.2		5.7		
4	41	42	43	42	41	41	43	44[a]/41	43.3±0.6	39.7±0.5	19.0	11.2	4.3
5	46	46				46							
6	52	53	54	55	54	53		53[a]/53		52.4±0.5		8.1	9.6
7	58	56				58	56		58.2±1.3		4.7		
	60												
	71												
	74	74											
8	78	79				79	80	80[a]/81	79.3±0.5	79.9±0.4	−0.8	−0.1	
9	83	83	82	81	82	83							2.3
9a	88	87	88						89.0±0.7		1.3		
10	93	92		92	92	93		91[a]/91					5.0
	98												
11	104	106	105	105		105		105[a]/					
12	116	118		117	117								
	123												
13	134	133	133	133	134	132	135	132[a]/132	135.1±0.3	132.2±0.4	0.9	1.7	2.8
14	142					176		177[a]/177		177.2±0.5		1.7	
15						181							
16	194	194	194	194	194	194		193[a]/194		193.6±0.3		1.3	2.6
17	200	199	198			200	197		197.3±0.4		1.3		
	205	204											
	219												
	227												
18	230	231	230	231	231	230		229[a]/229		229.0±0.1		4.0	4.4
19	239	240	240	240		238	238		238.4±0.7		4.4		
20	245	244				245							
21	249	250	250	248		250		249[a]/					
22	261	260	268	268		260							
23	281	280	278	279	278	281		278[a]/277		277.7±0.7		1.2	2.5
24	286	285					284		285.1±1.1		1.6		
	293												
	301												
	305												

[a]This value has been measured with the sample outside the diamond anvil.

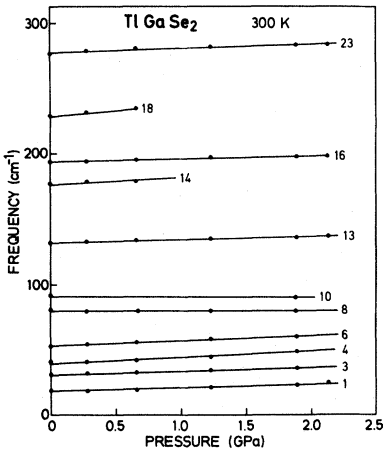

FIG. 7. Pressure dependence of the mode frequencies of $TlGaSe_2$ at 300 K. (Numbers correspond to the listing in Table IV.)

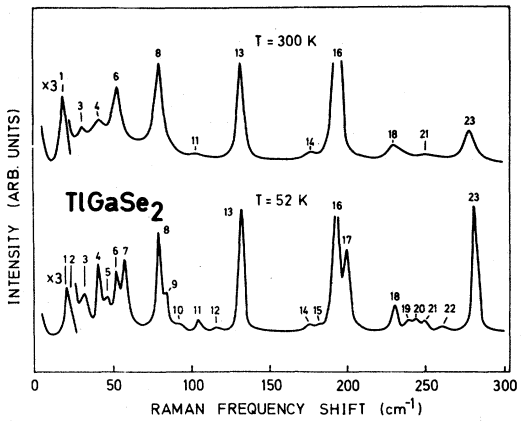

FIG. 9. Pressure dependence of the mode frequencies of $TlGaSe_2$ at 110 K. (Numbers correspond to the listing in Table IV.)

Fig. 8) as well as overlapping bands at atmospheric pressure (bands 3a and 3) can be seen. Vinogradov *et al.*[15] have pointed out that $TlGaSe_2$ and $TlGaS_2$, like GaSe, may crystallize in various polytypes depending on the growth techniques, and that this fact may lead to different results of the measurements. Comparison of our results with those of various other authors compiled in Table III for $TlGaS_2$ and in Table IV for $TlGaSe_2$ excludes the possibility that different polytypes of the substances have been investigated. The fact that some authors can resolve more bands (see Tables III and IV) may be due to their experimental conditions rather than having studied a polytype. In Ref. 14 the relative intensities of the bands in the Raman spectra of $TlGaS_2$ and $TlGaSe_2$ are listed. All bands not seen by other authors have weak intensities, which support the statement above.

We have observed evidence for a structural phase transition in $TlGaSe_2$ in the temperature dependence of the modes at zero applied pressure. In this experiment the sample was in the pressure cell with no applied pressure. The structural phase transition at low temperatures[12] is indicated by the sudden appearance of additional lines (Figs. 9 and 10). The occurrence of a structural phase transition in $TlGaSe_2$ at low temperatures has been confirmed by an x-ray investigation.[19]

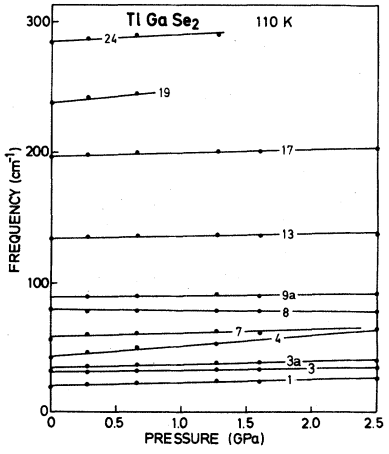

FIG. 8. Zero-pressure Raman spectrum of $TlGaSe_2$ at 300 and 52 K. (Numbers correspond to the listing in Table IV.)

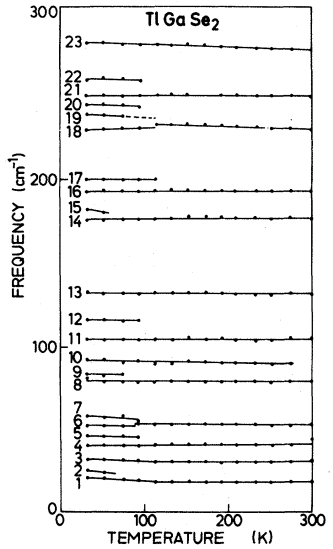

FIG. 10. Temperature dependence of the mode frequencies of $TlGaSe_2$ at zero pressure. (Numbers correspond to the listing in Table IV.)

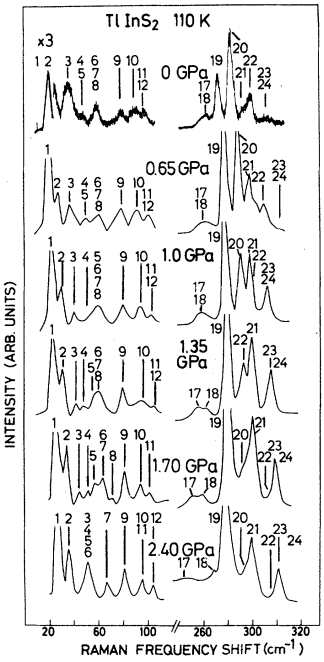

FIG. 11. Low- and high-frequency region of the Raman spectra of $TlInS_2$ at various pressures at 110 K. (Numbers correspond to the listing in Table V.)

Figures 11 and 12 show the Raman-active band of $TlInS_2$ at various pressures at 110 K. We have plotted the bands in the frequency region between 110 and 170 cm^{-1} in a separate figure (Fig. 12) to

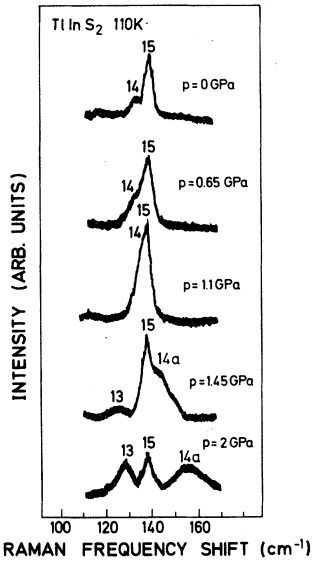

FIG. 12. Raman-active bands of $TlInS_2$ in the frequency region between 110 and 170 cm^{-1} at various pressures at 110 K. (Numbers correspond to the listing in Table V.)

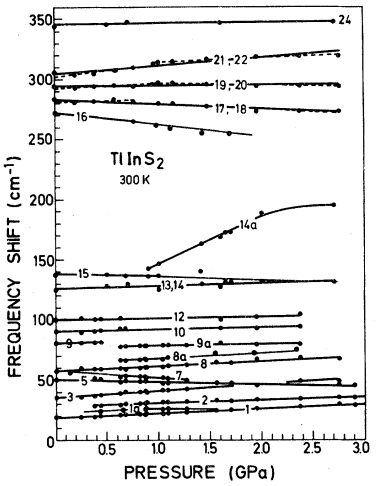

FIG. 13. Pressure dependence of the mode frequencies of $TlInS_2$ at 300 K. (Numbers correspond to the listing in Table V.)

bring out the details of the effect of pressure in this compound. As in the case of $TlGaS_2$ and $TlGaSe_2$, overlapping and crossing of bands are seen. In particular, the crossing of the bands 14 and 15 is to be noted (Fig. 12). In Figs. 13 and 14 the frequency shift of the various modes as a function of pressure at 300 and 110 K, respectively, are plotted, and in Table V the results are compared with those of other authors.

At both temperatures we see that the frequency shift of mode 14 increases drastically after the

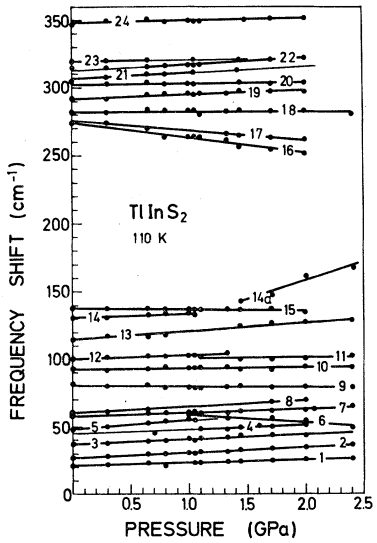

FIG. 14. Pressure dependence of the mode frequencies of $TlInS_2$ at 110 K. (Numbers correspond to the listing in Table V.)

TABLE V. Raman frequencies ν_i and $(1/\nu_i)(d\nu_i/dP)$ of the modes in β-$TlInS_2$ at low temperatures and at room temperature. ν_i^m are taken from our measurements. The values ν_i^c are determined by fitting the pressure data with a least-squares fit to $\nu_i(P)=\nu_i^c+(d\nu_i/dP)P$.

Number of the mode	ν_i (Ref. 10) (cm^{-1}) 300 K	ν_i (Ref. 14) (cm^{-1}) 300 K	ν_i (cm^{-1}) 110 K	ν_i (cm^{-1}) 300 K	ν_i (cm^{-1}) 110 K	ν_i (cm^{-1}) 300 K	$\frac{1}{\nu_i^c}\frac{d\nu_i}{dP}$ ($10^{-2}GPa^{-1}$) 110 K	$\frac{1}{\nu_i^c}\frac{d\nu_i}{dP}$ ($10^{-2}GPa^{-1}$) 300 K
1		19	22	19	21.2±0.4	18.7±0.2	10.0	21.2
1a						26.5±1.7		−0.2
2			28		27.0±0.3	28.5±0.3	14.4	9.6
3	35	36	38	35	37.0±0.4	35.4±0.3	9.8	16.3
4					44.6±1.3		7.3	
5		52	48	51	48.3±0.5	50.6±0.4	3.7	−3.3
6					64.8±2.4			
7			58		57.7±0.4	57.3±1.0	4.6	−9.2
8	57	60	61	59	60.5±0.3	57.7±0.4	7.4	7.5
8a						64.2±1.1		5.9
9	85	81	81	81	80.5±0.4	80.8±0.3	−0.8	2.5
9a						77.9±0.5		1.7
10		89	92	90	92.7±0.6	90.5±0.5	0.5	2.1
11					100.0±2.2		0.5	
12		100	100	100	100.3±0.4	100.2±0.6	3.0	1.4
13			117		115.1±0.9		5.3	
						126.0±1.3		2.0
14			132	125	131.2±0.7		1.9	
14a					103 ±9	106.0 ±2.1[b]	26.8	38.2[b]
15	137	138	138	137	138.3±0.4	138.1±0.4	−0.7	−1.0
16		272	273	269	274.0±1.2	272	−4.0	−3.4
17					275.6±0.9		−2.7	
						283.2±0.8[a]		−1.3[a]
18	279	281	280	282	282.2±0.8		0.2	
19	289	292	291	293	291.8±0.6		1.1	
						294.3±0.8[a]		0.2[a]
20		303	301	303	302.2±0.4		0.2	
21			307		306.7±0.3		1.4	
						304.5±1.1[a]		2.3[a]
22					311.8±0.8		1.6	
23			319		319.2±0.2		0.7	
24	343	346	348	347	348.0±0.5	345.8±0.7	0.5	0.3

[a]This value has been determined by a least-squares fit to all points.
[b]This value has been determined in the pressure range from 1.0—2.0 GPa where the mode shifts linearly with pressure. Above 2.0 GPa the pressure shift is nonlinear.

crossing and flattens again at pressures above 2 GPa at 300 K and 2.5 GPa at 110 K. Furthermore, modes with a negative pressure dependence are observed (Figs. 13 and 14) indicating an impeding phase transition at pressures above the maximum pressure of our measurements. In Fig. 13 the frequency shift versus pressure of some modes in the high-frequency region clearly shows a bending, indicated by the slopes of the dashed lines. One could argue that his may be connected with the strong pressure dependence of mode 14a and may be the indication of the occurrence of a phase transition. But looking at Fig. 14 we see that this bending of the frequency shift versus pressure is not seen at 110 K. Therefore, we think that the observed effect at 300 K is due to the overlap of two bands, causing the difficulty in locating the exact band positions. Similar features of the pressure dependence of some of the mode frequencies described above and displayed in Figs. 13 and 14 (mode 14a) are found in other molecular[20] and layer-structure crystals,[17] too. Thus, rather the absence of these features in the case of $TlGaS_2$ and $TlGaSe_2$ is peculiar. On the other hand, a compar-

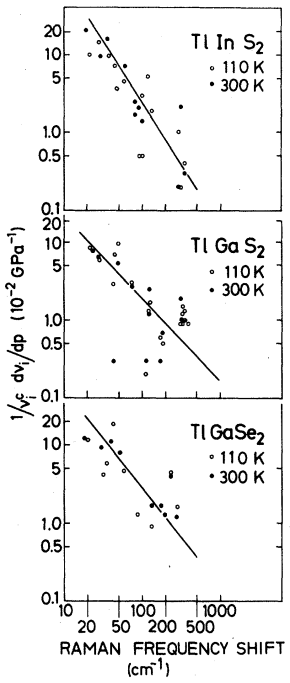

FIG. 15. Correlation between the logarithmic pressure coefficients of Raman-active phonons in $TlInS_2$, $TlGaS_2$, and $TlGaSe_2$ [$(1/\nu_i^c)(d\nu_i/dP)$ listed in Tables III, IV, and V].

ison of the properties of $TlGaSe_2$ and $TlInSe_2$ may give us some hints for a possible explanation. $TlInSe_2$ crystallizes at room temperature and atmospheric pressure in the tetragonal TlSe structure. Application of high pressure and high temperature [$p > 2$ GPa, $T > 600$ °C (Ref. 6)] transforms the monoclinic $TlGaSe_2$ exactly in this crystal structure. Thus, the features described above may be observed in $TlGaS_2$ and $TlGaSe_2$ at pressures much higher than the maximum pressures of the present measurements. This is further supported by comparing the pressure dependence of the modes of $TlInS_2$ in the pressure range below 1 GPa with that of the modes of $TlGaS_2$ and $TlGaSe_2$ in the larger pressure ranges.

We present in Fig. 15 a plot of $(1/\nu_i^c)(d\nu_i/dp)$ vs ν_i in a double logarithmic representation. Zallen[17] has pointed out that in molecular crystals the range of observed values of $(1/\nu_i)(d\nu_i/dp)$ reflects the range of force constants characterizing the solid. For molecular crystals Zallen as well as other authors[20,21] have shown that the gross behavior of $(1/\nu_i)(d\nu_i/dp)$ approximately follows $(1/\nu_i^c)(d\nu_i/dp) \sim \nu_i^{-2}$. Such a behavior was also found for orpiment (As_2S_3), a layer-structure crystal.[17] Figure 15 shows that only the frequencies of the Raman bands of $TlInS_2$ obey reasonably well such a relation. In the cases of $TlGaS_2$ and $TlGaSe_2$ the values of $(1/\nu_i)(d\nu_i/dp)$ are far from being frequency independent as would be expected, if Grüneisen approximations were true. On the other hand, the data reflect the existence of a hierarchy of force constants rather than only strong intralayer and weak interlayer binding in these compounds.

Krebs *et al.*[22] have measured the Raman-active modes of the adamantinelike anionic group (In_4S_{10}) in solutions and have found frequencies of 324, 317, and 289 cm^{-1} for the internal modes. Therefore, the modes above 300 cm^{-1} in $TlGaS_2$ and $TlInS_2$ are due to Ga-S and In-S vibrations, respectively. Replacing the S atom by the heavier Se atom in the X_4S_{10} polyhedra (X=Ga,In) under the assumption of only slightly changed force constants should decrease these mode frequencies, as can be observed in $TlGaSe_2$ (Figs. 7 and 8). Comparing $TlGaS_2$ and $TlInS_2$ (Figs. 5 and 14) we find a similar effect when the lighter Ga atom is replaced by the heavier In atom.

Until now the confusion of the structural data has prevented a factor-group analysis. All group-theoretical results were based on speculations and assumptions about the symmetry of a layer followed by the application of the correlation method to find the irreducible representations. Having more than *one* molecule or layer in the primitive cell the correlation method introduces the concept of Davydov splitting,[21] where the splitting of the Davydov components (equal to the number of molecules or layers in the primitive cell) depends on the strength of the interaction between the molecules and layers, respectively. In the case of $TlGaS_2$, $TlGaSe_2$, and $TlnS_2$, the components of the expected Davydov duplets have (A_g,A_u) and (B_g,B_u) symmetry, respectively. Now only the A_g and B_g modes are Raman-active, whereas the A_u and B_u modes are infrared-active.

This implies that the Raman spectra do not contain information about the Davydov splitting. We may point out that conclusions about Davydov splitting in earlier publications[12,15,16] were based on the assumption that the unit cell has *four* layers, which we have shown is not true. At the moment the available spectroscopic data do not allow exact conclusions about the Davydov splitting. On the other hand, a look at Fig. 2 as well as the fact that these crystals cleave easily into plates perpendicular to the c axis suggests that the interaction between the layers should be weak and the Davydov

splitting small.

Owing to the fact that the color of $TlInSe_2$ is already very dark at zero pressure we were only able to measure the pressure dependence of the A_{1g} phonon at 186 cm^{-1} at liquid-nitrogen temperature up to 1.6 GPa. We find a values of 1.0×10^{-2} GPa^{-1} for $(1/\nu)(d\nu/dP)$ of this mode.

V. SUMMARY

Contrary to earlier statements we have shown that the structure of $TlGaS_2$, $TlGaSe_2$, and $TlInS_2$ can be described in the space group $C2/c$. Our high-pressure Raman study supports the space-group assignment $C2/c$ (C_{2h}^6) with two layers per unit cell, as already mentioned by Vinogradov *et al.*[15]

Furthermore, our results show that there is a hierarchy of bonding forces rather than only strong intralayer and weak interlayer bonds. Our measurements reveal that the disappearance of Raman bands with increasing pressure are due to a crossing of modes of A_g and B_g symmetry. This shows that these features are necessary but not sufficient to indicate the occurrence of a structural phase transition. The fact that in $TlInS_2$ we find modes with a negative pressure dependence indicates an impending phase transition at pressures above the maximum pressure of our measurements. Our measurements of the temperature dependence of the modes of $TlGaSe_2$ at atmospheric pressure confirm the occurrence of a phase transition in this material at low temperature already reported by other authors.[12]

---

*Permanent address: Université de Sherbrooke, Sherbrooke, Québec, Canada.

†On leave from the University of Thessaloniki, Thessaloniki, Greece.

[1]H. Hahn, B. Wellmann, Naturwissenschaften 54, 42 (1967).

[2]G. D. Guseinov, A. M. Ramazanzade, E. M. Kerimova, and M. Z. Ismailov, Phys. Status Solidi 22, K117 (1967).

[3]D. Müller, G. Eulenberger, and H. Hahn, Z. Anorg. Allg. Chem. 398 207 (1973).

[4]D. Müller, F. E. Poltmann, and H. Hahn, Z. Naturforsch. 29b, 117 (1974).

[5]K.-J. Range, G. Engert, W. Müller, and A. Weiss, Z. Naturforsch. B 29, 181 (1974).

[6]K.-J. Range, G. Mahlberg, and S. Obenland, Z. Naturforsch. B 32, 1354 (1977).

[7]D. Müller and H. Hahn, Z. Anorg. Allg. Chem. 438, 258 (1978).

[8]T. I. Isaacs, J. Appl. Cryst. 6, 413 (1973).

[9]T. I. Isaacs and R. H. Hopkins, J. Cryst. Growth 29, 121 (1975).

[10]T. I. Isaacs and J. D. Feichtner, J. Solid State Chem. 14, 260 (1975).

[11]G. D. Guseinov, E. Mooser, E. M. Kerimova, R. S. Gamidov, I. V. Alekseev, and M. Z. Ismailov, Phys. Status Solidi 34, 33 (1969).

[12]K. Allakhverdiev, R. Sardarly, F. Wondre, and I. F. Ryan, Phys. Status Solidi B 88, K5 (1978).

[13]S. G. Abdullaeva, G. L. Belenkii, M. O. Godzhaev, and N. T. Mamedov, Phys. Status Solidi B 103, K61 (1981).

[14]N. M. Gasanly, B. N. Mavrin, Kh. E. Sterin, V. I. Tagirov, and Z. D. Khalafov, Phys. Status Solidi B 86, K49 (1979).

[15]E. A. Vinogradov, G. N. Zhizhin, N. N. Melnik, S. I. Subbotin, V. V. Panfilov, K. R. Allakhverdiev, E. Yu. Salaev, and R. Kh. Nani, Phys. Status Solidi B 95, 383 (1979).

[16]K. R. Allakhverdiev, M. A. Nizametdinova, R. M. Sardarly, E. A. Vinogradov, G. N. Zhizhin, in *Proceedings of the International Conference on Lattice Dynamics, Paris, 1977,* edited by M. Balkanski (Flammarion Paris, 1978), p. 95.

[17]R. Zallen, Phys. Rev. B 9, 4485 (1974).

[18]G. I. Piermarini, S. Block, J. D. Barnett, and R. A. Forman, J. Appl. Phys. 46, 2774 (1975).

[19]J. Ihringer, H. D. Hochheimer, and H. G. v. Schnering (unpublished).

[20]T. Chattopadhyay, C. Carlone, A. Jayaraman, and H. G. v. Schnering, Phys. Rev. B 23, 2471 (1981).

[21]R. Zallen and M. L. Slade, Phys. Rev. B 18, 5775 (1978).

[22]B. Krebs, H. M. Hurter, D. Voelker, and H. J. Wallstab, Z. Kristallogr. 154, 63 (1980), and private communications.